High-pressure Synthesis and Characterization of the Alkali Metal Borate HP-RbB_3O_5

Gerhard Sohr[a], Stephanie C. Neumair[b] and Hubert Huppertz[a]

[a] Institut für Allgemeine, Anorganische und Theoretische Chemie, Leopold-Franzens-Universität Innsbruck, Innrain 80 – 82, A-6020 Innsbruck, Austria

[b] Tyrolit Schleifmittelwerke Swarovski K.G., Swarovskistraße 33, A-6130 Schwaz, Austria

Reprint requests to H. Huppertz. E-mail: Hubert.Huppertz@uibk.ac.at

Z. Naturforsch. **2012**, *67b*, 1197 – 1204 / DOI: 10.5560/ZNB.2012-0248
Received August 4, 2012

The rubidium triborate HP-RbB_3O_5 (HP = high-pressure) was synthesized under high-pressure/high-temperature conditions of 6 GPa and 1000 °C in a Walker-type multianvil apparatus. The precursor was gained from a mixture of rubidium carbonate Rb_2CO_3 and boric acid H_3BO_3 heated at 850 °C under normal pressure conditions. The single-crystal structure determination showed that HP-RbB_3O_5 is isotypic to HP-KB_3O_5, crystallizing monoclinically with eight formula units in the space group $C2/c$ possessing the lattice parameters $a = 982.3(2)$, $b = 885.9(2)$, $c = 919.9(2)$ pm, and $\beta = 104.0(1)°$. The boron-oxygen framework consists of trigonal-planar BO_3 groups as well as corner- and edge-sharing BO_4 tetrahedra that are connected to a three-dimensional framework. Therein, the rubidium cations are surrounded by 10 oxygen anions. IR- and Raman-spectroscopic investigations were performed on single crystals of the compound.

Key words: High Pressure, Borate, Crystal Structure

Introduction

In the literature, the system Rb-B-O exhibits twelve different oxoborates with nine different constitutions. With the composition RbB_5O_8, three different polymorphs are known: a high-temperature modification α-RbB_5O_8 [1], a low-temperature phase β-RbB_5O_8 [2], and the metastable phase γ-RbB_5O_8 [3], which was obtained by quenching samples from 380 °C. With the formula RbB_3O_5, a low-temperature phase α-RbB_3O_5 [4] and a high-temperature phase β-RbB_3O_5 [5] are known. For all other compositions, solely one compound exists in each case: $Rb_5B_{19}O_{31}$ [6], $Rb_3B_3O_6$ [7], $Rb_2B_4O_7$ [8], RbB_9O_{14} [3], $Rb_2B_8O_{13}$ [3], $Rb_4B_{10}O_{17}$ [9], and Rb_3BO_3 [10]. Four different synthetic strategies were used to obtain these phases. A common route is drying an aqueous solution of rubidium carbonate and boric acid until dehydrated products are obtained. A second alternative is the direct reaction of a mixture of dried Rb_2CO_3 with pure B_2O_3 in a solid-state reaction. The third option is the crystallization of a glass, and as a fourth variant, one can find the synthesis of α-$RbBO_2$ from rubidium carbonate and boron nitride [7]. Interestingly, none of the known rubidium borates was obtained through high-pressure experiments.

Generally, the structures of these normal-pressure borates are built up from trigonal BO_3 groups and BO_4 tetrahedra. In contrast, high-pressure borates often exhibit an increasing amount of tetrahedrally coordinated boron atoms. Even the structural motif of two edge-sharing BO_4 tetrahedra forming a B_2O_6 group is possible under high-pressure conditions, as first discovered in $Dy_4B_6O_{15}$ [11]. Meanwhile several other high-pressure phases are known to contain this B_2O_6 group, *e. g.* $RE_4B_6O_{15}$, (RE = Dy, Ho) [11, 12], α-$RE_2B_4O_9$ (RE = Sm, Eu, Gd, Tb, Ho) [13, 14], HP-MB_2O_4 (M = Ni [15], Co [16]), β-FeB_2O_4 [17], $Co_7B_{24}O_{42}(OH_2)\cdot 2H_2O$ [18], and HP-KB_3O_5 [19]. Besides these high-pressure phases, the recently discovered compound $KZnB_3O_6$ [20, 21] is the only normal-pressure phase exhibiting the structural element of two edge-sharing BO_4 tetrahedra. Accordingly, high-pressure conditions favor the formation of tetrahedrally coordinated boron atoms, the edge-sharing of BO_4 tetrahedra, an increased coordination

number of the bridging oxygen atoms ($O^{[3]}$), and often an enhanced coordination of the metal cations as can be expected from the pressure coordination rule [22]. The new compound HP-RbB_3O_5 fulfills these expectations being isotypic to HP-KB_3O_5 [19] and representing the fourteenth borate containing edge-sharing BO_4 tetrahedra. Furthermore, HP-RbB_3O_5 is the fourth high-pressure alkali metal borate in the recently synthesized series HP-LiB_3O_5 [23], HP-$Na_2B_4O_7$ [24] and HP-KB_3O_5 [19]. This paper reports about the synthesis, the single-crystal structure determination, and the vibrational spectroscopic investigations of HP-RbB_3O_5 in comparison to the isotypic phase HP-KB_3O_5.

Experimental Section

Synthesis

HP-RbB_3O_5 was obtained by a two-stage synthesis during a systematic scanning of the system Rb-B-O under high-pressure/high-temperature conditions. A stoichiometric mixture of 1 mol Rb_2CO_3 (99.9 %, ChemPUR, Karlsruhe/Germany) and 6 mol H_3BO_3 (99.5 %, Merck, Darmstadt/Germany) was filled into a FKS 95/5 (feinkornstabilisiert, 95 % Pt, 5 % Au) crucible (No. 21, Ögussa, Wien/Austria), heated to 850 °C in 6 h, cooled down to 600 °C in 12 h, and then quenched to room temperature. The resulting product was finely ground, filled into a crucible made of hexagonal boron nitride (HeBoSint® P100, Henze BNP GmbH, Kempten/Germany), built into an 18/11-assembly and compressed by eight tungsten carbide cubes (TSM-10, CERATIZIT Austria GmbH, Reutte/Austria). A hydraulic press (mavo press LPR 1000-400/50, Max Voggenreiter GmbH, Mainleus/Germany) and a Walker-type module (also Max Voggenreiter GmbH) were used to apply the pressure. Details of the assembly are described in the references [25 – 29]. The precursor was compressed to 6 GPa within three hours and kept at this pressure during the heating period. The sample was heated to 1000 °C in 10 min and kept at this temperature for 10 min. After cooling to 480 °C within 40 min, the reaction mixture was quenched to room temperature. The decompression of the assembly lasted nine hours.

The octahedral pressure medium (MgO, Ceramic Substrates & Components Ltd., Newport, Isle of Wight/UK) was recovered and broken apart. The sample was separated from the surrounding boron nitride crucible showing two phases: the first containing colorless crystals and a second, dark phase (presumably carbon). The colorless crystals were found to be HP-RbB_3O_5. This compound is stable in air for several days.

Crystal structure analysis

The powder diffraction pattern was obtained in transmission geometry, using a Stoe Stadi P powder diffractometer with Ge(111)-monochromatized MoK_{α_1} radiation (λ = 70.93 pm). The diffraction pattern showed reflections of HP-RbB_3O_5 and hexagonal BN from the crucible that could not be removed completely. Fig. 1 shows the experimental powder pattern that matches well with the theoretical pattern simulated from the single-crystal data. Single crystals of HP-RbB_3O_5 were isolated by mechanical fragmentation. The single-crystal intensity data were collected at room temperature using a Nonius Kappa-CCD diffractometer with graphite-monochromatized MoK_α radiation (λ = 71.073 pm). A semi-empirical absorption correction based on equivalent and redundant intensities (SCALEPACK [30]) was applied to the intensity data. All relevant details of the data collection and evaluation are listed in Table 1. The monoclinic space group $C2/c$ was derived from the systematic extinctions. The structural refinement was performed with the positional parameters of HP-KB_3O_5 as starting values, since the two phases are isotypic (full-matrix least-squares on F^2, SHELXL-97 [31, 32]). All atoms were

Table 1. Crystal data and structure refinement of HP-RbB_3O_5 (standard deviations in parentheses).

Empirical formula	HP-RbB_3O_5
Molar mass, g mol^{-1}	197.9
Crystal system	monoclinic
Space group	$C2/c$
Single crystal diffractometer	Enraf-Nonius Kappa CCD
Radiation; wavelength, pm	MoK_α; 71.073
Single-crystal data	
a, pm	982.3(2)
b, pm	885.9(2)
c, pm	919.9(3)
β, deg	104.0(1)
V, Å^3	776.7(3)
Formula units per cell, Z	8
Calculated density, g cm^{-3}	3.39
Crystal size, mm^3	0.05 × 0.10 × 0.11
Temperature, K	293(2)
F(000), e	736
Absorption coefficient, mm^{-1}	12.7
Absorption correction	multi-scan [30]
θ range, deg	3.1 – 37.8
Range in hkl	$-16 \rightarrow 14$, ± 15, ± 15
Total no. of reflections	6894
Independent reflections/R_{int}/R_σ	2083/0.0464/0.0391
Reflections with $I > 2\sigma(I)$	1724
Data/ref. parameters	2083/83
Goodness-of-fit on F^2	1.035
Final $R1/wR2$ [$I > 2\sigma(I)$]	0.0343/0.0778
$R1/wR2$ (all data)	0.0452/0.0825
Largest diff. peak/hole, e Å^{-3}	1.42/ − 1.53

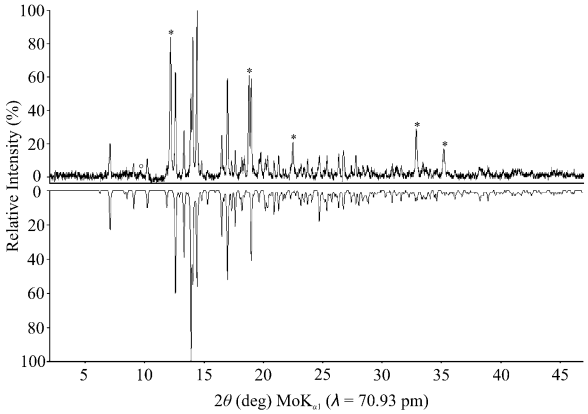

Fig. 1. Experimental powder pattern (top), compared with the theoretical powder pattern of HP-RbB_3O_5 (bottom), simulated from single-crystal data. Additional reflections marked with an asterisk are caused by hexagonal boron nitride from the crucible that could not be removed completely. The reflection marked with a circle could not be explained.

refined with anisotropic displacement parameters. The final difference Fourier syntheses did not reveal any significant peaks. Tables 2 – 4 list the positional parameters, anisotropic displacement parameters, and selected interatomic distances.

Further details of the crystal structure investigation may be obtained from Fachinformationszentrum Karlsruhe, 76344 Eggenstein-Leopoldshafen, Germany (fax: +49-7247-808-666; E-mail: crysdata@fiz-karlsruhe.de, http://www.fiz-karlsruhe.de/request_for_deposited_data.html) on quoting the deposition number CSD-424931.

Table 2. Atomic coordinates (Wyckoff positions 8*f* for all atoms) and equivalent isotropic displacement parameters U_{eq} (Å^2) of HP-RbB_3O_5 (space group: *C*2/*c*) with standard deviations in parentheses. U_{eq} is defined as one third of the trace of the orthogonalized U_{ij} tensor.

Atom	*x*	*y*	*z*	U_{eq}
Rb1	0.07635(2)	0.34537(2)	0.44463(2)	0.01589(8)
B1	0.2033(2)	0.0073(2)	0.2368(2)	0.0068(3)
B2	0.3206(2)	0.2503(2)	0.1797(2)	0.0076(3)
B3	0.4261(2)	0.4615(2)	0.0673(2)	0.0068(3)
O1	0.0820(2)	0.0085(2)	0.0977(2)	0.0080(2)
O2	0.1553(2)	0.0582(2)	0.3649(2)	0.0077(2)
O3	0.2452(2)	0.3497(2)	0.24301(2)	0.0095(2)
O4	0.3153(2)	0.0975(2)	0.2022(2)	0.0081(2)
O5	0.4089(2)	0.3026(2)	0.0956(2)	0.0093(2)

Vibrational spectroscopy

The ATR-FT-IR (*A*ttenuated *T*otal *R*eflection) spectra of single crystals of HP-RbB_3O_5 were measured in the spectral range of 600 – 4000 cm^{-1} with a Bruker Vertex 70 FT-IR spectrometer (spectral resolution 4 cm^{-1}) equipped with a MCT (*M*ercury *C*admium *T*elluride) detector and attached to a Hyperion 3000 microscope. As mid-infrared source, a Globar (silicon carbide) rod was used. A frustum-shaped germanium ATR crystal with a tip diameter of 100 μm was pressed on the surface of the borate crystal to crush it into small pieces of μm-size. 32 scans of the sample were ac-

Atom	U_{11}	U_{22}	U_{33}	U_{12}	U_{13}	U_{23}
Rb1	0.0187(2)	0.0138(2)	0.0187(2)	−0.00203(6)	0.01147(8)	−0.00022(6)
B1	0.0085(7)	0.0056(7)	0.0072(7)	−0.0006(6)	0.0034(6)	0.0005(5)
B2	0.0089(8)	0.0065(7)	0.0080(7)	−0.0001(6)	0.0032(6)	−0.0008(6)
B3	0.0088(7)	0.0073(7)	0.0055(7)	−0.0003(6)	0.0038(6)	0.0008(5)
O1	0.0069(5)	0.0125(5)	0.0051(5)	−0.0016(4)	0.0022(4)	0.0011(4)
O2	0.0106(5)	0.0066(5)	0.0073(5)	−0.0006(4)	0.0047(4)	−0.0012(4)
O3	0.0125(6)	0.0060(5)	0.0127(6)	−0.0016(4)	0.0080(5)	−0.0021(4)
O4	0.0092(5)	0.0054(5)	0.0107(5)	−0.0012(4)	0.0048(4)	0.0006(4)
O5	0.0121(6)	0.0064(5)	0.0119(6)	0.0003(4)	0.0075(5)	0.0010(4)

Table 3. Anisotropic displacement parameters (Å^2) of HP-RbB_3O_5 (space group: *C*2/*c*) with standard deviations in parentheses.

Rb1–O5	273.1(2)	B1–O2	144.3(3)	B2–O3	136.9(3)	B3–O2	141.5(3)
Rb1–O3a	277.1(2)	B1–O4	145.6(3)	B2–O4	137.2(3)	B3–O5	144.9(3)
Rb1–O2a	280.8(2)	B1–O3	148.2(3)	B2–O5	137.4(3)	B3–O1a	152.4(3)
Rb1–O2b	291.8(2)	B1–O1	152.3(3)			B3–O1b	154.6(3)
Rb1–O4a	294.0(2)						
Rb1–O4b	320.5(2)	∅ B1–O	147.6	∅ B2–O	137.2	∅ B3–O	148.4
Rb1–O3b	321.2(2)						
Rb1–O1a	334.5(2)						
Rb1–O1b	343.1(1)						
Rb1–O3c	344.7(2)					B3···B3	223.1(3)
∅ Rb1–O	308.1					Rb1···Rb1	339.6(1)

Table 4. Interatomic distances (pm) in HP-RbB_3O_5 (space group: *C*2/*c*) calculated with the single-crystal lattice parameters (standard deviations in parentheses).

quired. A correction for atmospheric influences using the OPUS 6.5 software was performed.

The single-crystal Raman spectra of HP-RbB_3O_5 were measured in the spectral range of 100 – 1600 cm^{-1} with a Raman micro-spectrometer LabRAM HR-800 (HORIBA JOBIN YVON) and hundredfold magnification. The length of the crystal was approximately 0.35 mm. As excitation source, a Nd:YAG laser ($\lambda = 532.22$ nm) was used. To avoid destruction of the crystal, the laser beam was weakened by a D 0.6 filter. The Raman-scattered light was detected through an optical grid with 1800 lines mm^{-1}. Two ranges were measured with a spectral resolution better than 2 cm^{-1}. The measurement time per step was 300 s. A background correction was applied.

Results and Discussion

Synthetic conditions

HP-RbB_3O_5 could be synthesized over a wide range of starting compositions (molar ratio $Rb_2CO_3 : H_3BO_3$ from 4 : 1 to 1 : 12), a wide pressure range (4 – 10 GPa), and at temperatures of 700 – 1000 °C. A detailed schedule of all performed syntheses, including molar ratios, reaction conditions, and products is shown in Table 5. The side product represented by the dark inclusions, which are not detectable *via* powder X-ray diffraction measurements, is presumably carbon, arising from the rubidium carbonate.

Crystal structure of HP-RbB_3O_5

The structure of HP-RbB_3O_5 is built up from BO_3 groups as well as corner- and edge-sharing BO_4 tetrahedra as presented in Fig. 2. A detailed description can be found in ref. [19]. The isotypy to HP-KB_3O_5 indicates that there are no large differences between the two structures. Table 6 compares the unit cells, the coordination numbers of the alkali metal ions, and the average bond lengths. The coordination numbers of the specific atoms as well as their connection patterns are the same.

The boron-oxygen distances inside the corner-sharing tetrahedra of HP-RbB_3O_5 vary between 144.3(3) and 152.3(3) pm with a mean value of 147.6 pm, being slightly smaller than those in HP-KB_3O_5 (144.7(2) – 152.4(2) pm with a mean value of 147.7 pm). With distances of 136.9(3) – 137.4(3) pm and a mean value of 137.2 pm, the trigonal BO_3

Table 5. List of experiments performed to prepare HP-RbB_3O_5.

Rb_2CO_3	:	B_2O_3	p (GPa)	T (°C)	Result
8	:	1	4	700	HP-RbB_3O_5
8	:	1	6	1000	HP-RbB_3O_5
1	:	2	2	800	amorphous
1	:	2	3	1000	amorphous
1	:	2	4	800	HP-RbB_3O_5
1	:	2	6	1000	HP-RbB_3O_5
1	:	2	6	700	HP-RbB_3O_5
1	:	2	10	1000	HP-RbB_3O_5
1	:	3	6	1000	HP-RbB_3O_5
1	:	4	10	1000	HP-RbB_3O_5
1	:	6	3	1000	amorphous
1	:	6	6	1000	HP-RbB_3O_5
1	:	6	6	700	$RbB_5O_6(OH)_4 \cdot 2H_2O$
1	:	6	10	1000	HP-RbB_3O_5

Table 6. Comparison of the isotypic structures HP-KB_3O_5 and HP-RbB_3O_5.

Empirical formula	HP-KB_3O_5	HP-RbB_3O_5
Molar mass, g mol^{-1}	151.53	197.90
Unit cell dimensions		
a, pm	960.8(2)	982.3(2)
b, pm	877.0(2)	885.9(2)
c, pm	909.9(2)	919.9(2)
β, deg	104.4(1)	104.0(1)
V, nm^3	0.7428(3)	0.7767(3)
Coordination number (CN)		
$M1$ (M = K, Rb)	10	10
Interatomic distances		
av. $M1$–O (M = K, Rb) distance, pm	300	308.1
av. B–O distance in [BO_3] groups, pm	137.3	137.2
av. B–O distance in [BO_4] groups, pm	147.7	148.0
B···B distance in the B_2O_2 ring, pm	221.5(1)	223.1(3)

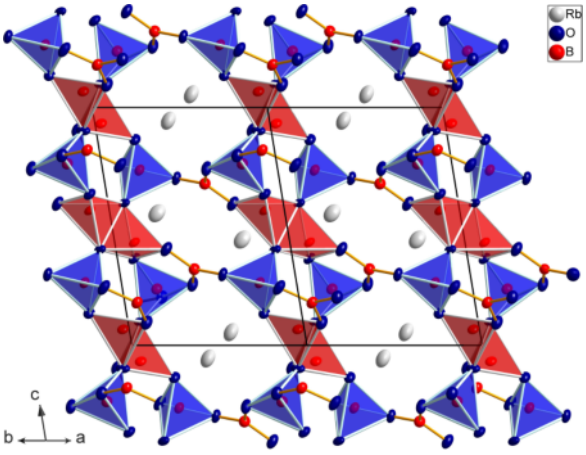

Fig. 2 (color online). Projection of the crystal structure of HP-RbB_3O_5 along [110]. Spheres: 90 % displacement ellipsoides.

Table 7. Values of the interatomic distances (pm) and interatomic angles (deg) in the B_2O_6 groups of different borates.

Compound	OBO_{in}	BOB_{in}	$d_{B\text{-}O1}$	$d_{B\text{-}O2}$	$d_{B\text{-}O3}$	$d_{B\text{-}O4}$	OBO_{out}	$d_{B\cdots B}$
$Dy_4B_6O_{15}$	94.1	85.9	153.3	150.7	146.1	145.4	109.2	207.2
$Ho_4B_6O_{15}$	94.4	85.6	153.6	151.1	145.6	144.3	109.7	207
α-$Sm_2B_4O_9$	92.7	87.3	150.3	149.8	147.9	142.4	113.6	207.1
α-$Eu_2B_4O_9$	94	86	150.1	148.3	148.6	143	113.6	205.3
α-$Gd_2B_4O_9$	94	86	149.9	148.2	148.3	142.7	113.5	204
α-$Tb_2B_4O_9$	93.9	86.1	149.4	147.7	147.8	142.2	113.5	205.5
α-$Ho_2B_4O_9$	94.2	85.7	150.8	149.1	147.8	142.6	114.2	204
HP-NiB_2O_4	93.6	86.4	153	151.6	144.5	144.3	114.7	208.8
β-FeB_2O_4	93.4	86.6	152.5	151.2	144.3	144.3	113.8	208.3
HP-CoB_2O_4	93.3	86.7	152.8	151.7	144.4	144.2	114.2	209
$KZnB_3O_6$	92	88	150.9	148.4	145.4	144.9	114	207.9
$Co_7B_{24}O_{42}(OH)_2{\cdot}2H_2O$	90.6	89	155.4	150.9	148	144.7	110.9	214.8
HP-KB_3O_5	87.2	92.7	154.8	151.4	144.6	141.2	114.8	221.5
HP-RbB_3O_5	86.2	93.2	154.6	152.4	144.9	141.5	113.9	223.1

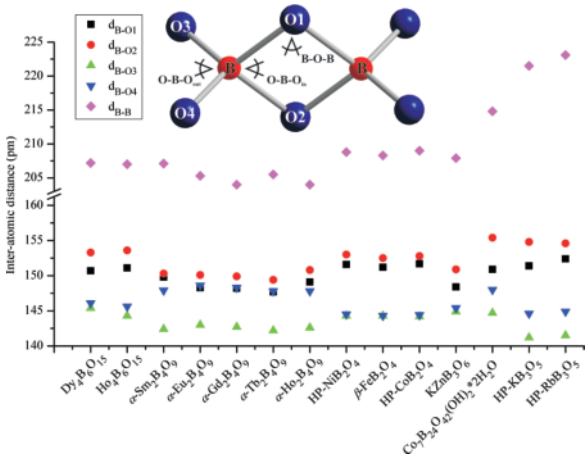

Fig. 3 (color online). Comparison of the interatomic distances in the B_2O_6 groups of different borates with edge-sharing BO_4 tetrahedra.

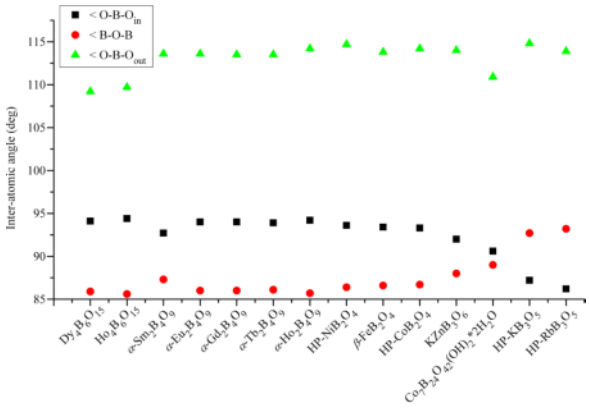

Fig. 4 (color online). Comparison of the interatomic angles in the B_2O_6 groups of different borates possessing edge-sharing BO_4 tetrahedra.

groups also show slightly smaller boron-oxygen distances than the corresponding ones in HP-KB_3O_5 (137.1(2) – 137.9(2) pm, mean value 137.3 pm). The edge-sharing tetrahedra exhibit boron-oxygen distances between 141.5(3) and 154.6(3) pm with a mean value of 148.4 pm. All mean values of the boron-oxygen distances correspond well with the known average values for B–O distances in BO_4 (147.6 pm) and BO_3 (137.0 pm) groups [33 – 35].

In Figs. 3 and 4 and in Table 7, the distances, angles, and specific values within the B_2O_6 group of HP-RbB_3O_5 are compared with the corresponding values of all other phases containing such groups. Fig. 3 also shows the assignment used for this comparison. With a value of 223.1(3) pm, HP-RbB_3O_5 reveals the longest B···B distance of all structures possessing edge-sharing BO_4 tetrahedra. Since the B–O distances are comparable in all different B_2O_6 groups, the long B···B distance is caused by a shrinking of the angle O–B–O_{in}, while the angle B–O–B_{in} is widened. The angle O–B–O_{out} is hardly affected by this scissor motion. The tricoordinated oxygen atom at the common edge, that only occurs in the compounds HP-KB_3O_5 and HP-RbB_3O_5 so far, induces the scissor motion.

The rubidium atoms are situated in channels along [110] and are coordinated by 10 oxygen atoms with interatomic distances between 273.1(2) and 344.7(2) pm and an average distance of 308.1 pm (Fig. 5). The next oxygen atom has a distance of 371.1 pm. The distance between two neighboring Rb^+ cations is 339.6(1) pm. The shortest Rb–O and Rb···Rb distances are smaller than those reported for other phases in the system Rb–B–O (*e. g.* $Rb_2B_4O_7$: Rb–O_{min} = 275 pm, Rb···Rb_{min} = 357 pm [8]; β-RbB_3O_5: Rb–O_{min} = 284 pm, Rb···Rb_{min} = 393 pm [5]; $Rb_5B_{19}O_{31}$: Rb–

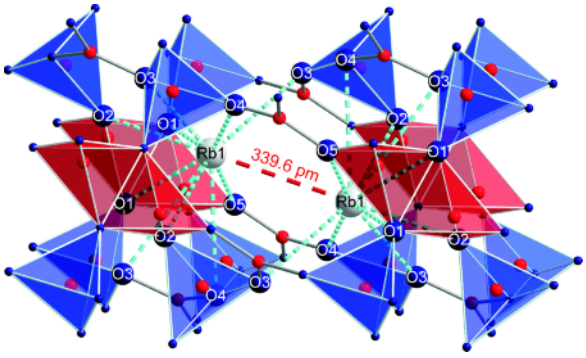

Fig. 5 (color online). Coordination of the Rb1 ion (short dashed bonds) in HP-RbB_3O_5 together with the distance to the neighboring Rb1 atom (long dashed bond).

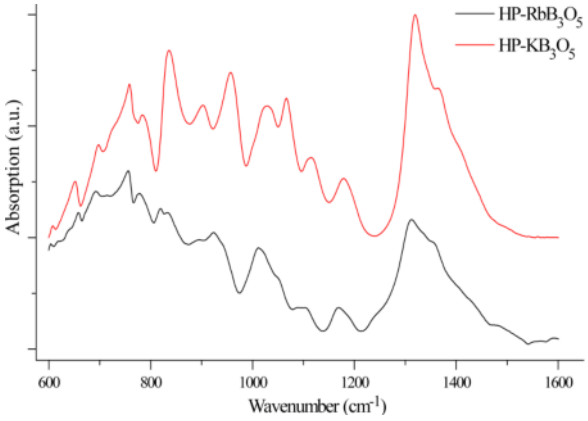

Fig. 6 (color online). Single-crystal ATR-FT-IR spectra of HP-RbB_3O_5 and HP-KB_3O_5.

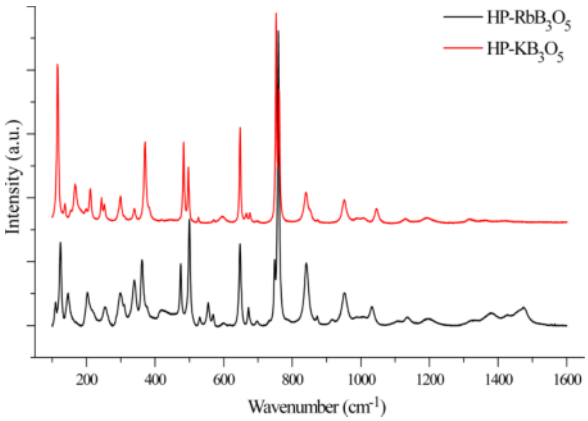

Fig. 7 (color online). Single-crystal Raman spectra of HP-RbB_3O_5 and HP-KB_3O_5.

$O_{min} = 276.6$ pm, $Rb{\cdots}Rb_{min} = 376.5$ pm [6]). The coordination number of 10 is the highest in the system Rb-B-O and so far only achieved in β-RbB_5O_8 [2]. Normally, the coordination number varies between 6 and 9.

The bond-valence sums of the individual cations and anions of HP-RbB_3O_5 were calculated from the crystal structure, using the bond-length/bond-strength concept (ΣV) [36, 37]. The calculation revealed a value of +1.38 for Rb1. For the boron ions, the values are 3.00 (B1), 2.98 (B2), and 3.03 (B3). The oxygen ions show values in the range of −1.84 to −2.12. The values fit to the formal charges of the ions. The bond-valence sums can also be calculated using the CHARDI (*Char*ge *D*istribution in Solids, ΣQ) concept [38, 39], leading to values of +0.98 (Rb1), +3.00 (B1), +2.98 (B2), +3.03 (B3), −1.84 (O1), −2.12 (O2), −2.01 (O3), −2.00 (O4), and −2.04 (O5). These values are in good accordance with the values calculated for HP-KB_3O_5. For both compounds, the values of O1 are slightly lower than expected. This can be explained by the fact that O1 is the tricoordinated oxygen atom at the common edge of the two BO_4 tetrahedra in both compounds.

Furthermore, the MAPLE values (*Ma*delung *P*art of *L*attice *E*nergy) [40–42] of HP-RbB_3O_5 were calculated to compare them with the MAPLE values received from the summation of the binary components Rb_2O [43] and the high-pressure modification B_2O_3-II [44]. The value of 34 156 kJ mol^{-1} was obtained in comparison to 34 104 kJ mol^{-1} (deviation = 0.15 %), starting from the binary oxides [Rb_2O (2393 kJ mol^{-1}) + B_2O_3-II (21 938 kJ mol^{-1})].

Vibrational spectroscopy

The FTIR-ATR and the Raman spectra of HP-RbB_3O_5 and HP-KB_3O_5 are compared in Figs. 6 and 7. For borates in general, bands in the region of 800 – 1100 cm^{-1} usually apply to B–O stretching modes of boron atoms, which are tetrahedrally coordinated to oxygen atoms [45, 46], while absorption bands at 1200 – 1450 cm^{-1} are expected for borates containing BO_3 groups [46, 47].

For HP-KB_3O_5, the harmonic vibrational frequencies at the Γ point were calculated [19]. Based on these calculations, a more specific assignment of both, the IR and the Raman bands of HP-RbB_3O_5 was possible. Above 1320 cm^{-1}, mainly the corner-sharing BO_3 groups are oscillating. Between 1215 and 950 cm^{-1},

stretching vibrations of the corner- and edge-sharing BO_4 tetrahedra occur. Bands of bending and complex vibrations of both BO_3 and BO_4 units are located between 905 and 200 cm^{-1}. Below 185 cm^{-1}, lattice vibrations involving the alkali metal ions occur [19].

In the ATR-FTIR spectrum of HP-RbB_3O_5, several groups of absorption bands of the boron-oxygen tetrahedra were detected between 700 and 1135 cm^{-1}. The BO_3 modes appear between 1250 and 1500 cm^{-1}. Furthermore, weak OH or water bands are observed in the range of 3000 to 3500 cm^{-1}. The Raman spectrum shows lattice vibrations between 100 and 185 cm^{-1}, complex and bending vibrations of BO_3 and BO_4 groups from 200 to 700 cm^{-1}, and vibrations of the BO_4 tetrahedra from 950 to 1215 cm^{-1}. Above 1215 cm^{-1}, the oscillation of the BO_3 groups can be seen. It has to be considered that all boron-oxygen units are linked to other boron-oxygen units. Hence, every motion inside of one boron-oxygen unit induces motions in the connected units. However, according to calculations for HP-KB_3O_5, ATR-bands around 1001, 1070, and 1105 cm^{-1} may be assigned to the edge-sharing tetrahedra, along with Raman peaks at 1013, 1161, 1205, and 1213 cm^{-1} [19]. The weak intensity of the ATR bands between 3000 and 3500 cm^{-1} changed with time. No corresponding bands could be seen in the Raman spectrum, so the bands presumably arise from surface water.

Conclusions

With the synthesis of HP-RbB_3O_5, the first isotypic compound to HP-KB_3O_5 was synthesized and characterized. The structure consists of BO_3 groups as well as corner- and edge-sharing BO_4 tetrahedra. Interestingly, HP-RbB_3O_5 forms at a higher pressure (6 GPa) than HP-KB_3O_5 (3 GPa). It is the second compound possessing all known basic structural motifs of borates in one structure. The system Cs-B-O is the last alkali metal boron oxygen system without any high-pressure borate known so far. Therefore, the synthesis of a high-pressure caesium borate will be the subject of our future efforts.

Acknowledgement

Special thanks go to Univ.-Prof. Dr. R. Stalder (University of Innsbruck) for performing the IR measurements, to L. Perfler (University of Innsbruck) for the Raman measurements and to Dr. G. Heymann for the recording of the single-crystal data set.

[1] R. S. Bubnova, I. G. Polyakova, Y. E. Anderson, S. K. Filatov, *Glass Phys. Chem.* **1999**, *25*, 183.
[2] N. Penin, L. Seguin, M. Touboul, G. Nowogrocki, *J. Solid State Chem.* **2001**, *161*, 205.
[3] J. Krocher, *Bull. Soc. Chim. Fr.* **1968**, *3*, 919.
[4] M. G. Krzhizhanovskaya, Y. K. Kabalov, R. S. Bubnova, E. V. Sokolova, S. K. Filatov, *Crystallogr. Rep.* **2000**, *45*, 572.
[5] M. G. Krzhizhanovskaya, R. S. Bubnova, V. S. Fundamenski, I. I. Bannova, I. G. Polyakova, S. K. Filantov, *Crystallogr. Rep.* **1998**, *43*, 21.
[6] M. G. Krzhizhanovskaya, R. S. Bubnova, I. I. Bannova, S. K. Filatov, *Crystallogr. Rep.* **1999**, *44*, 187.
[7] S. Schmid, W. Schnick, *Acta Crystallogr.* **2004**, *C60*, i69.
[8] M. G. Krzhizhanovskaya, R. S. Bubnova, I. I. Bannova, S. K. Filatov, *Crystallogr. Rep.* **1997**, *42*, 226.
[9] P. Tolédano, *Bull. Soc. Chim. Fr.* **1966**, *7*, 2302.
[10] R. S. Bubnova, M. G. Krzhizhanovskaya, V. B. Trofimov, I. G. Polyakova, S. K. Filatov, *Abstracts VII Conference on Crystal Chemistry of Inorganic and Coordination Compounds* **1995**, 97.
[11] H. Huppertz, B. von der Eltz, *J. Am. Chem. Soc.* **2002**, *124*, 9376.
[12] H. Huppertz, *Z. Naturforsch.* **2003**, *58b*, 278.
[13] H. Emme, H. Huppertz, *Chem. Eur. J.* **2003**, *9*, 3623.
[14] H. Emme, H. Huppertz, *Acta Crystallogr.* **2005**, *C61*, i29.
[15] J. S. Knyrim, F. Roessner, S. Jakob, D. Johrendt, I. Kinski, R. Glaum, H. Huppertz, *Angew. Chem. Int. Ed.* **2007**, *46*, 9097.
[16] S. C. Neumair, R. Kaindl, H. Huppertz, *Z. Naturforsch.* **2010**, *65b*, 1311.
[17] S. C. Neumair, R. Glaum, H. Huppertz, *Z. Naturforsch.* **2009**, *64b*, 883.
[18] S. C. Neumair, R. Kaindl, H. Huppertz, *J. Solid State Chem.* **2012**, *185*, 1.
[19] S. C. Neumair, S. Vanicek, R. Kaindl, D. M. Többens, C. Martineau, F. Taulelle, J. Senker, H. Huppertz, *Eur. J. Inorg. Chem.* **2011**, *27*, 4147.
[20] S. Jin, G. Cai, W. Wang, M. He, S. Wang, X. Chen, *Angew. Chem. Int. Ed.* **2010**, *49*, 4976.
[21] Y. Wu, J. Y. Yao, J. X. Zhang, P. Z. Fu, Y. C. Wu, *Acta Crystallogr.* **2010**, *E66*, i45.

[22] A. Neuhaus, *Chimia* **1964**, *18*, 93.
[23] S. C. Neumair, S. Vanicek, R. Kaindl, D. M. Többens, K. Wurst, H. Huppertz, *J. Solid State Chem.* **2011**, *184*, 2490.
[24] S. C. Neumair, G. Sohr, S. Vanicek, K. Wurst, R. Kaindl, H. Huppertz, *Z. Anorg. Allg. Chem.* **2012**, *638*, 81.
[25] N. Kawai, S. Endo, *Rev. Sci. Instrum.* **1970**, *41*, 1178.
[26] D. Walker, M. A. Carpenter, C. M. Hitch, *Am. Mineral.* **1990**, *75*, 1020.
[27] D. Walker, *Am. Mineral.* **1991**, *76*, 1092.
[28] D. C. Rubie, *Phase Transitions* **1999**, *68*, 431.
[29] H. Huppertz, *Z. Kristallogr.* **2004**, *219*, 330.
[30] Z. Otwinowski, W. Minor in *Methods in Enzymology*, Vol. 276, *Macromolecular Crystallography*, Part A (Eds.: C. W. Carter Jr, R. M. Sweet), Academic Press, New York, **1997**, pp. 307.
[31] G. M. Sheldrick, SHELXL-97, Program for the Refinement of Crystal Structures, University of Göttingen, Göttingen (Germany) **1997**.
[32] G. M. Sheldrick, *Acta Crystallogr.* **2008**, *A64*, 112.
[33] E. Zobetz, *Z. Kristallogr.* **1990**, *191*, 45.
[34] F. C. Hawthorne, P. C. Burns, J. D. Grice in *Boron: Mineralogy, Petrology and Geochemistry*, (Ed.: E. S. Grew), Mineralogical Society of America, Washington, **1996**.
[35] E. Zobetz, *Z. Kristallogr.* **1982**, *160*, 81.
[36] N. E. Brese, M. O'Keeffe, *Acta Crystallogr.* **1991**, *B47*, 192.
[37] I. D. Brown, D. Altermatt, *Acta Crystallogr.* **1985**, *B41*, 244.
[38] R. Hoppe, *Z. Kristallogr.* **1979**, *150*, 23.
[39] R. Hoppe, S. Voigt, H. Glaum, J. Kissel, H. P. Müller, K. Bernet, *J. Less-Common Met.* **1989**, *156*, 105.
[40] R. Hoppe, *Angew. Chem., Int. Ed. Engl.* **1966**, *5*, 95.
[41] R. Hoppe, *Angew. Chem., Int. Ed. Engl.* **1970**, *9*, 25.
[42] R. Hübenthal, MAPLE, Program for the Calculation of Distances, Angles, Effective Coordination Numbers, Coordination Spheres, and Lattice Energies, University of Gießen, Gießen (Germany), **1993**.
[43] P. Touzain, M. Caillet, *Rev. Chim. Miner.* **1971**, *8*, 277.
[44] C. T. Prewitt, R. D. Shannon, *Acta Crystallogr.* **1968**, *B24*, 869.
[45] J. P. Laperches, P. Tarte, *Spectrochim. Acta* **1966**, *22*, 1201.
[46] M. Ren, J. H. Lin, Y. Dong, L. Q. Yang, M. Z. Su, L. P. You, *Chem. Mater.* **1999**, *11*, 1576.
[47] W. C. Steele, J. C. Decius, *J. Chem. Phys.* **1956**, *25*, 1184.